Percolation in insect nest networks: Evidence for optimal wiring

Sergi Valverde,[1,2] Bernat Corominas-Murtra,[1] Andrea Perna,[2] Pascale Kuntz,[3] Guy Theraulaz,[2] and Ricard V. Solé[1,4]
[1]*ICREA-Complex Systems Laboratory, Universitat Pompeu Fabra, Dr. Aiguader 80, 08003 Barcelona, Spain*
[2]*CRCA, Université Paul Sabatier, CNRS-UMR 5169, 118 Route de Narbonne, 31062 Toulouse, France*
[3]*Ecole Polytechnique de Nantes, BP50609, 44306 Nantes, France*
[4]*Santa Fe Institute, 1399 Hyde Park Road, New Mexico 87501, USA*
(Received 22 July 2008; revised manuscript received 7 March 2009; published 12 June 2009)

Optimization has been shown to be a driving force for the evolution of some biological structures, such as neural maps in the brain or transport networks. Here we show that insect networks also display characteristic traits of optimality. By using a graph representation of the chamber organization of termite nests and a disordered lattice model, it is found that these spatial nests are close to a percolation threshold. This suggests that termites build efficient systems of galleries spanning most of the nest volume at low cost. The evolutionary consequences are outlined.

DOI: 10.1103/PhysRevE.79.066106 PACS number(s): 89.75.Fb, 89.75.Hc, 87.18.−h

I. INTRODUCTION

An important question in the study of evolution concerns the relevance of optimization as a driving force shaping living matter in relation to path dependence or structural constraints [1]. Biological structures, from proteins to brains, display different levels of adaptation to their environmental context. Sometimes, such adaptive traits are tied to optimal designs. An example is provided by treelike transport networks such as blood vessels [2]. For this class of distribution networks, it has been shown that some basic assumptions such as the self-similar nature of the branching tree and energy minimization explain the observed architectures. Here, scaling arguments allow us to understand a wide range of phenomena spanning many orders of magnitude. Similarly, brains are known to display optimal wiring, resulting from the metabolic cost associated to cognitive tasks [3–5].

The case for insect nests is a much less known example. Although building is by far the most spectacular outcome of insect societies, the exact rules of building are largely unknown [6]. Termite nests in particular are one of the most obvious examples and their properties and organization are an important component of their ecological success. Termites are known to be the earliest evolving social insects and true ecosystem engineers, deeply affecting their habitats [7]. Their nests are excellent examples of large scale designs, buffering external fluctuations and providing the backbone for all colony activities. These nest structures can be described in terms of complex networks [8]. This type of structure emerges as the outcome of the collective dynamics within colonies formed by more or less large groups of individuals with fairly limited cognitive capacities [9–11]. As it occurs with many biological and technological networks, they have neither completely regular nor completely random topology [12,13]. Most of these networks display the small-world (SW) effect, which makes them efficiently connected. Even if spatially embedded networks can display SW patterns [14], but in general they do not reach the SW behavior due to geometrical constraints [15]. For example, we cannot easily connect distant nodes if there is a maximal link length and nodes are located far from each other. Link competition for available space also limits the number of shortcuts. Planar networks, for example, do not allow link crossings. These limitations suggest that the general small-world model needs to be extended. In that case, how are spatial networks optimized through evolution?

The study of average statistical patterns in termite nests has shown that these networks seem to minimize connectivity [8]. Actually, the analysis of network sensitivity to link removal reveals that the elimination of single node (a corridor in the real nest) is enough to disconnect the network in more than 40% of the cases. These observations point toward some optimal design of nest organization. Our goal in this paper is to provide a theoretical framework to explain the origins of such patterns within the context of percolation transition in spatial lattices. In this context, as it happens with cortical maps [16], bone networks [17,18], or artificial designed circuits [19], the type of termite nests studied here [20] displays a characteristic layered architecture. As will be shown below, such layered structure provides a good framework to understand their global organization and the presence of optimality.

Our approach is based on a simple model of disordered lattice with link removal and node merging. Here, node location disorder introduces a certain fraction of so-called *shortcuts*, that is, links that do not belong to the corresponding three-dimensional (3D) Delaunay triangulation [21]. We study the transport properties of the network realization and the functional role played by shortcuts. In addition, closely interacting nodes are merged into a single hub gathering all the connections from participating nodes. Merging enables a transition from regular deterministic networks to spatially embedded random networks and appears to be an indispensable ingredient for modeling termite networks.

The paper is organized as follows. In Sec. II, the basic data sets are presented. In Sec. III our disordered lattice model is introduced and compared with data sets. We obtain the best fit parameter sets through an optimization method described in Sec. IV. Mean field approximation to the average degree is presented in Sec. V. The topological efficiency of these nests is measured in Sec. VI and our results are summarized in Sec. VII.

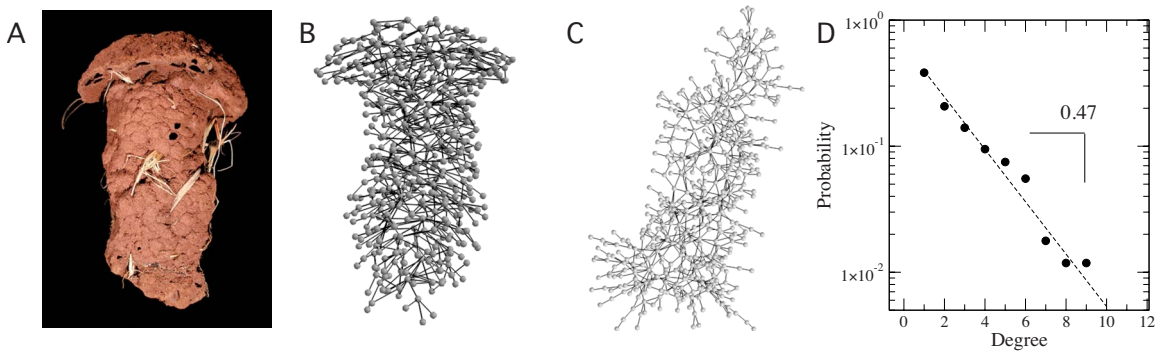

FIG. 1. (Color online) Cubitermes nest define a 3D very sparse network with nodes representing chambers and links depicting galleries. Here we show a (a) photograph of the real Cubitermes nest ($c9$), (b) the spatial 3D network organization, and (c) the topological organization of the network shown in a 2D layout (see text). These networks are homogeneous, following an exponential degree distribution as shown in (d).

II. TERMITE NETWORK MAPPING

Six *Cubitermes* nests [see Fig. 1(A)] were used. The nests, labeled M9–M12, M18, and M19, originated from different locations in Central African Republic and Cameroon. One of the nests, M19, was still under construction when it was collected. All the nests comprise several chambers interconnected by openings and short corridors.

Nests were imaged and reconstructed into 3D virtual volumes using x-ray tomography with a medical scanner. For every nest, we obtain the transportation network $G=(V,E)$ corresponding to the biggest set of physically interconnected chambers in the original nest. In this network, a node $v \in V$ represents a physical chamber and a link $\{v_i,v_j\} \in E$ depicts a physical corridor between chambers v_i and v_j.

The network G was obtained with standard image processing techniques as follows:

(i) *Binarization.* In the tomographical images, denser materials (e.g., the nest walls) are represented by lighter gray levels; soft materials and air are characterized by significantly darker gray levels. The volumetric images were binarized by applying a threshold on the gray-level value of the voxel (the 3D equivalent of a pixel). Now, white voxels mark the nest scaffold and black voxels represent air (chambers and corridors). Given the naturally high contrast offered by the material no edge enhancement algorithm was applied.

(ii) *Threshold on distance from nest walls.* Cubitermes nests consist of relatively big chambers connected by narrow corridors (less than ~ 0.5 mm in radius). Hence each voxel that is more than 0.5 mm away from any of the walls either belongs to a chamber or to the space outside the nest. We detected and individually labeled all the connected sets of voxels in the empty space whose distance from the walls was bigger than two voxels (D26 distance). Each connected numbered component marks the "core" of a single nest chamber and its label and properties were recorded into a network node.

(iii) *Constrained dilation of chambers.* The chamber cores were concurrently dilated, one step at a time, to fill progressively their surrounding empty space (stopping at walls). At some point, a dilated core also crams into its outgoing corridors and gets in touch with the others dilated cores coming from the other end of the corridor. In this case, an edge between the vertices was created, corresponding to the physical corridor.

As a result of this process of network extraction, the graph associated to the nest structure is obtained [see Figs. 1(B) and 1(C)]. Termite nests are homogeneous networks that follow an exponential degree distribution [see Fig. 2(D)],

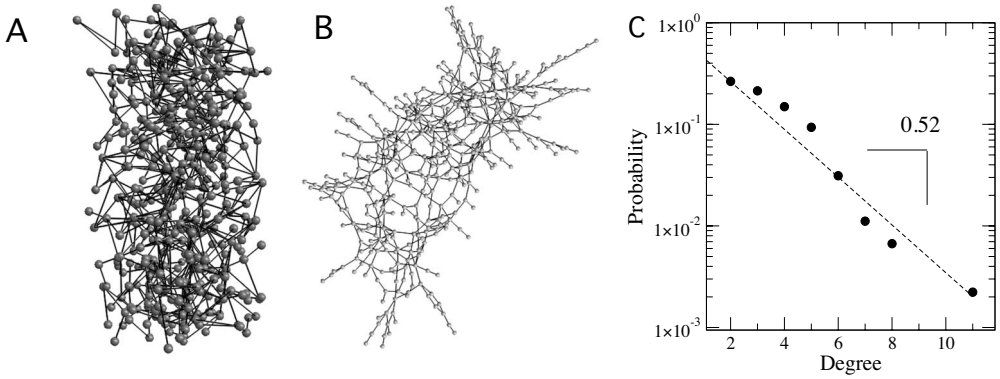

FIG. 2. Illustration of the synthetic networks generated with our model. (a) 3D organization of the network. (b) Topological organization. (c) Probability degree distribution is exponential. Parameters: $L=6$, $H=14$, $1-p=0.46$, $1-q=0.5$, $\delta=0.96$, and $\epsilon=0.75$. The bending at low k values [not seen in \] is due to the latticelike behavior exhibited by our model.

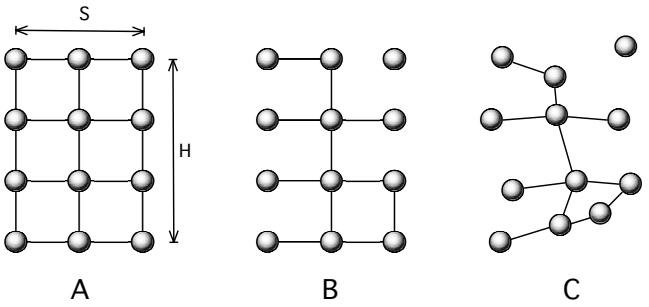

FIG. 3. 2D illustration for the construction rules used in the disordered lattice model. (a) Our model starts from an isotropic 3D lattice with S^2H nodes. Here, $H=4$ and $S=3$. (b) Layered structures can be simulated if $p>q$, where p is the survival probability of horizontal (intralayer) link and q is the survival probability of vertical (interlayer) links. (c) Node jittering deforms the original lattice and yields a nonhomogeneous spatial node distribution.

$$P(k) = \frac{1}{\gamma}\exp\left(-\frac{k}{\gamma}\right), \tag{1}$$

where $\gamma \approx 0.45$ [8].

III. LATTICE MODEL

Here, we investigate the topological and geometrical features of Cubitermes nests with a network model of link removal and merging on a disordered lattice. Our construction network model consists of four different steps:

(1) We start from a fully connected 3D lattice $G=(V,E)$ with $|V|=S^2H$ nodes, where every node has four horizontal links and two vertical links. The model assumes a 3D lattice constructed of H horizontal layers having S^2 nodes each [see Fig. 3(A)]. Without loss of generality, we place any pair of adjacent lattice nodes at a distance equal to 1.

(2) From the above lattice, we perform a random (asymmetric) link deletion process. The following algorithm was used: (i) a random lattice node u is chosen. (ii) Pick a random link attached to the node u and remove this horizontal (vertical) link with probability $p(q)$. Iterate steps (i)–(ii) until there are only $2(S-1)SHp$ horizontal links and $S^2(H-1)q$ vertical links.

(3) Node locations are jittered with a 3D random displacement $[-\delta,\delta]$ of size $0\leq\delta\leq 1$ [see Fig. 3(C)].

(4) Node merging rule: (1) choose a random pair $\{i,j\} \in E$ of linked nodes i and j. (2) The nodes i and j are merged together to the node i of degree $k_i(t+1)=k_i(t)+k_j(t)-2$ if the Euclidian distance is $d(i,j)<\epsilon$ (see Fig. 4). Perform (1) and (2) until the separation distance between all pairs of linked nodes is above the threshold ϵ.

Figure 3 illustrates the different stages involved in our network model. Every layer has a uniform bond density denoted by $p\leq 1$, that is, the probability of having a bond connecting two adjacent nodes within the same layer (or *intralayer* density). On the other hand, there is a different *interlayer* density $q\leq 1$ of edges connecting nodes in different vertically adjacent layers [see Fig. 3(B)]. This model is roughly equivalent to a multilayered structure [22] having alternating layers with different concentrations p and q. Depending on the relative ratio p/q we will obtain asymmetric structures with a vertical (horizontal) main direction or a symmetric structure with no predominant direction.

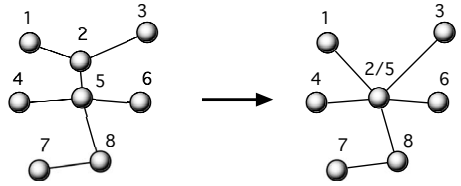

FIG. 4. Node merging. The last step in our model merges any pair of nodes falling apart less than ϵ units (see text). Here, we merge nodes 2 and 5 and remove the edge {2, 5}. Merging of two nodes in a graph causes a reduction in the degree of any node that had been adjacent to both.

However, we will rarely see such an ordered structure in termite nests. We can obtain a (more realistic) disordered structure when node locations are perturbed by adding an individual random displacement of size $0\leq\delta\leq 1$ [see Fig. 3(C)]. This geometrical perturbation causes topological disorder by interacting with the node merging rule.

Node merging enables the emergence of hub nodes having many more connections than the rest of nodes. Indeed, this is the case for ant and termite tunneling networks [23–26]. The merging of two nodes causes a reduction in the number of nodes and links in the graph (when $\delta>0$).

IV. OPTIMAL PARAMETER SETS

In this section, we describe the fitting method to obtain the best model parameters for every Cubitermes network. We can estimate the characteristic separation between adjacent lattice nodes with the average link length in the network

$$\langle l_{ij}\rangle = \frac{1}{N(N-1)}\sum_{i\neq j} l_{ij}, \tag{2}$$

where link length l_{ij} is the (Euclidean) distance between nodes i and j. Lattice dimensions S and H can be computed from the enclosing network volume divided by the characteristic length $\langle l_{ij}\rangle$ (see Fig. 5),

$$S = \frac{\max(x_i)-\min(x_i)}{\langle l_{ij}\rangle} \tag{3}$$

and

$$H = \frac{\max(y_i)-\min(y_i)}{\langle l_{ij}\rangle}, \tag{4}$$

where (x_i,y_i,z_i) are the coordinates of the ith node. We compute the tightest enclosing 3D box that minimizes the empty volume (i.e., places without network nodes) [27] or, alternatively, the lattice that minimizes the approximation error. When the network is not perfectly aligned with the vertical direction (Z axis) we can rotate the node coordinates with the three orthogonal eigenvectors e_1,e_2,e_3, weighted by the corresponding eigenvalues $\lambda_1,\lambda_2,\lambda_3$.

It is very difficult to find an analytical estimate for the remaining lattice parameters p, q, δ, and ϵ. In this case, we

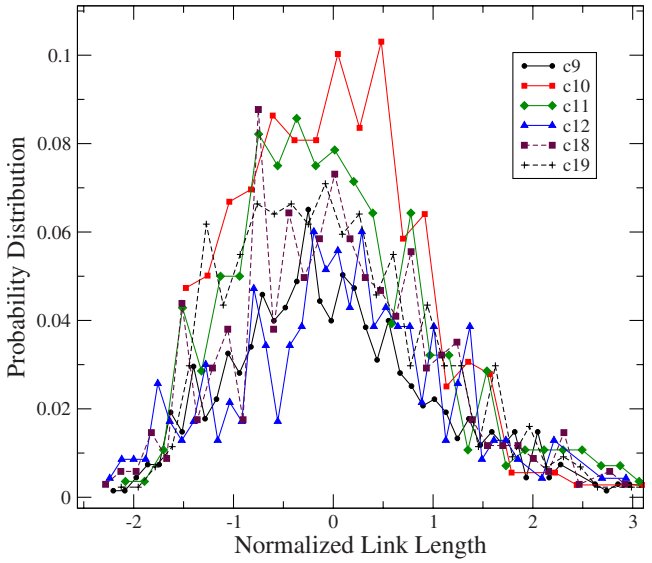

FIG. 5. (Color online) Plots of link length distributions $P(l_{ij})$ for the termite nests analyzed here. Distributions have been rescaled by subtracting the average link length $\langle l_{ij} \rangle$ divided by the standard deviation. All the distributions show a well-defined mean value.

can search the entire space of lattice networks with an evolutionary algorithm [28] for the set of parameters that provides the best model fitting to the target network. One possible set of constraints to be imposed is based on local properties. It has been suggested a classification of different networks by means of the set of k-subgraph frequencies (or subgraph census) [29]. When looking at different networks, we find that their internal structure in terms of small subgraphs differs considerably. This suggests a way to distinguish between networks having distinct features using their subgraph census as the network signature. This is done by Vazquez *et al.* [30] who used the abundance of triples and four-node loops measured from a real protein network to obtain the best model parameters. Here, we will compute the four-subgraph census [31] to estimate the approximation error of model networks when compared to the real networks. Then, we will use the four-node subgraph frequencies to guide our genetic search algorithm and obtain the best estimates for p, q, δ, and ϵ.

Here, we minimize the distance U between the subgraph census measured in the target network and the predicted subgraph census measured in the model network,

$$U = \left[\sum_{m} (P(m) - P'(m))^2 \right]^{1/2} \left(1 + \frac{|C - C'|}{C + C'} \right), \qquad (5)$$

where $P(m)$ is the probability of the subgraph m in the real network, $P'(m)$ is the probability of the subgraph m in the model network, C is the number of different (nonzero) subgraphs in the real network, and C' is the number of different subgraphs in the model network. The rightmost term ensures the synthetic network will have the same number of nonzero four subgraphs as the real target network. It can be easily shown that the above corresponds to a well-behave metric definition concerning the motif distribution.

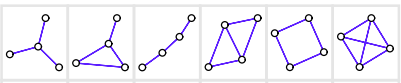

C9	2276	300	5532	11	48	n/a
C10	590	7	1037	n/a	1	n/a
C11	858	12	1349	n/a	4	n/a
C12	832	42	1603	1	21	n/a
C18	758	83	1710	6	5	n/a
C19	1841	723	4259	79	56	6

FIG. 6. (Color online) Four-subgraph census for the six termite networks analyzed in this paper. From top to bottom, the different networks have $C=5$, $C=4$, $C=4$, $C=5$, $C=5$, and $C=6$ different nonzero four subgraphs. Note that the most frequent motifs are the four stars and the four chains. In order to generate realistic multilayered networks is important to be able to reproduce the least frequent motifs too.

Figure 6 shows the subgraph census for the six networks analyzed here. We can see that $4 \leq C \leq 6$ and the most abundant subgraphs are the four stars and the four chains. Still, the less frequent subgraphs signal important deviations to be captured by the specific values of lattice parameters. Table I summarizes the best fit parameters found with our algorithm for the termite networks.

We have exhaustively explored the four-dimensional (4D) parameter space (defined by p, q, δ, ϵ) to assess the reliability of our fitting method. In Fig. 7(A) we show the metric landscape for the termite nest $c18$ as a function of p and q when (δ, ϵ) is fixed. This surface shows there is a unique global minimum that coincides with the best fitting parameters found with our evolutionary search algorithm. Other termite nests exhibit similar metric surfaces with unique global minima (not shown). In addition, the model networks minimizing the distance U with the target nest also reproduce a number of observed topological properties, including the average number of links per node L/N [see Fig. 7(B)]. Note that we can reproduce the same average connectivity although is not explicitly accounted for by our metric definition [see Eq. (5)]. We will show below that we can reproduce other nonlocal network properties (see Sec. VI).

TABLE I. Best fitting parameters for the Cubitermes networks analyzed here (see text). For all networks, the fitting error is $U \approx 0.01$.

Nest	N	$\langle k \rangle$	S	H	$1-p$	$1-q$	δ	ϵ
$c9$	507	2.66	6	14	0.566	0.522	0.965	0.751
$c10$	349	2.056	4	21	0.54	0.719	0.544	0.884
$c11$	260	2.153	4	16	0.505	0.928	0.735	0.923
$c12$	183	2.54	4	11	0.524	0.538	0.56	0.94
$c18$	287	2.38	5	11	0.455	0.704	0.596	0.939
$c19$	268	3.26	4	16	0.188	0.469	0.449	0.804

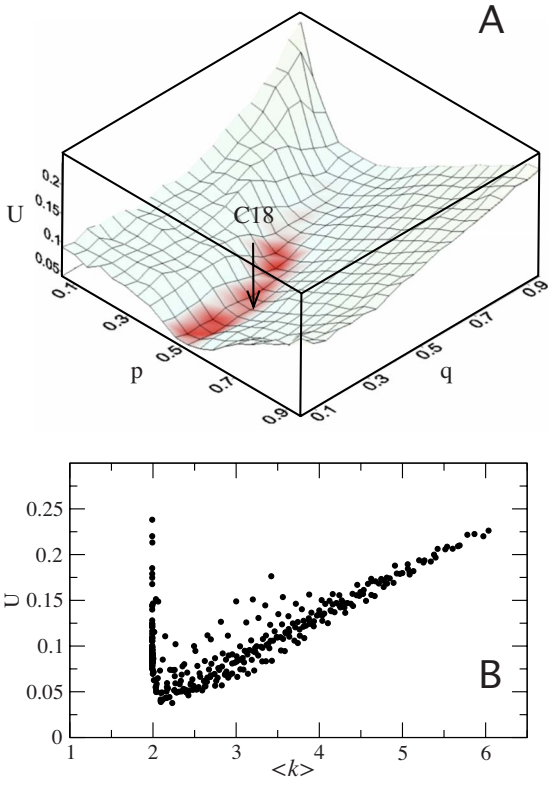

FIG. 7. (Color online) Exploration of the parameter space for the disordered lattice model. Average metric distance U between synthetic networks and the $c18$ termite network as a function of (a) (p,q) and (b) the average number of links $\langle k\rangle$. The arrow in (a) denotes the global minimum found by the evolutionary search algorithm. This minimum is located in the region of the parameter space with $U\leq 0.07$ (in dark gray and in red). In addition, the plot in (b) shows how the model network minimizing the distance U with the $c18$ nest also has the same connectivity $\langle k\rangle\approx 2.38$ (see Table I). Plots obtained from numerical simulations by taking 20 sample networks for each (p,q) (2000 networks). The parameters $\delta=0.59$ and $\epsilon=0.39$ were fixed to the best fitting parameters found in Table I for $c18$.

V. $\langle k\rangle$ ESTIMATION

In previous sections we have presented our network data sets, the lattice model, and how to fit model parameters in order to reproduce the observed architectures. In this section, we will proceed to analyze the optimization conjecture by developing a mean field theory estimate of the average degree $\langle k\rangle$. Such theory allows defining a percolation condition which can be compared with the observed data sets.

The average degree, $\langle k\rangle$, is negatively affected by the deletion of links. On the other hand, merging reduces the number of nodes, thus increasing the average number of links per node. Corrections of higher order introduce the possibility of more complex merging, which could result again not only in a loss of nodes but also in a loss of links. The analytic derivation of $\langle k\rangle$ considers two terms. The first term introduces the effect of merging within connected nodes, resulting in a net increase in $\langle k\rangle$, whereas the second introduces the fusion of links, thus relaxing the increase in $\langle k\rangle$ through node merging. It is important to recall that, within a lattice, average connectivities lower than 2 would correspond to linear chains. Since we deal with more complex structures, our computations are valid for $\langle k\rangle>2$. Furthermore, we make the assumption that all nodes within a layer are connected regardless of link removal.

Let us consider a lattice where a process of jittering and merging is performed with probabilities δ and ϵ, respectively. Let $\pi(\delta,\epsilon)$ be the probability that a randomly chosen node is merged with another given node. Let v_i be the set of points which are a distance equal or less than $\delta+\epsilon$ from the geometrical location of the node i in the ordered lattice and v_j be the set of points which are a distance $d\leq\delta$ from the node j in the ordered lattice. Then, the general form of $\pi(\delta,\epsilon)$ is

$$\pi(\delta,\epsilon)=\frac{1}{2}\int_{v_i\cap v_j}dv\left(\int_{v_i\cup v_j}dv\right)^{-1}. \tag{6}$$

(The term 1/2 arises because when merging at work, from two nodes we form a single node.) Now, three different cases can be considered:

Case 1. The first observation is that if

$$2\delta+\epsilon\leq 1, \tag{7}$$

$\pi(\delta,\epsilon)=0$ since $v_i\cap v_j=\emptyset$.

In this situation, the number of nodes will be fixed, $N=HS^2$ (i.e., all the nodes of the lattice). The number of expected links will be

$$|E(p,q)|=(2p+q)HS^2-2pHS-qS^2, \tag{8}$$

given that

$$\langle k\rangle=\frac{2|E(p,q)|}{N} \tag{9}$$

we obtain, by defining $x\equiv 4p+2q$,

$$\langle k\rangle\approx x+\mathcal{O}\left(\frac{1}{S}+\frac{1}{H}\right). \tag{10}$$

Case 2. The next situation considers that $\sqrt{2}\geq 2\delta+\epsilon>1$. This combination of parameters enables the merging process to be at work. The probability of merging will be proportional to the volume of the intersection between two spheres of radius $\delta+\epsilon$ and δ, centered, for example, in (0,0,0) and (1,0,0), respectively. Notice that if $\sqrt{2}\geq 2\delta+\epsilon>1$, only merging between two connected nodes will occur. Let us call this probability $\pi_1(\delta,\epsilon)$. Given a node i the only nodes susceptible to be merged are the nodes j directly connected to it. Applying Eq. (6), we obtain $\pi_1(\delta,\epsilon)$ for our case by solving the following integrals:

$$\int_{v_i\cup v_j}dv=\frac{4}{3}\pi(\epsilon+\delta)^3+\frac{4}{3}\pi\delta^3-\int_{v_i\cap v_j}dv,$$

$$\int_{v_i\cap v_j}dv=\frac{\pi}{12}(2\delta+\epsilon-1)^2(1+4\delta+2\epsilon-3\epsilon^2).$$

(The last integral is obtained by computing the intersection volume between two spheres of different radius.) The num-

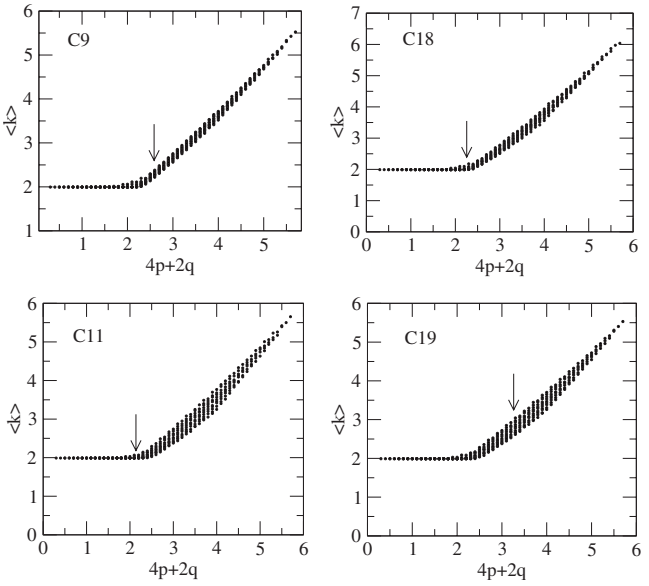

FIG. 8. Plots of average degree $\langle k\rangle$ of the largest connected component vs expected connectivity $4p+2q$ in synthetic networks. There is a nonlinear transition from the sparsest network with $\langle k\rangle=2$ to the maximal connectivity $\langle k\rangle=6$. The arrows indicate the location of the real termite network (see Sec. V). We can appreciate that $c9$, $c11$, and $c18$ are close to the percolating transition while $c19$ is not because of its relatively large average degree (see text).

ber of nodes of the net in this first approach, $N(\delta,\epsilon)$, will be

$$N(\delta,\epsilon)\sim[1-\pi_1(\delta,\epsilon)]HS^2. \tag{11}$$

Consistently with the proposed methodology, we also expect that horizontal (vertical) links are present with probability $p(q)$. The expected number of links $|E(p,q)|$ will satisfy Eq. (8) by using the appropriate values of p and q. Thus, we can compute the average degree,

$$\langle k\rangle \approx \frac{(4p+2q)HS^2-4pHS-2qS^2}{[1-\pi_1(\delta,\epsilon)]HS^2} = \frac{x}{[1-\pi_1(\delta,\epsilon)]}+\mathcal{O}\left(\frac{1}{S}+\frac{1}{H}\right). \tag{12}$$

As in the first case, we observe the linear character of the leading term of the above equation (see Fig. 8 for comparison with numerical results).

Case 3. Now we explore the scenario where $2\geq 2\delta+\epsilon>\sqrt{2}$. This is interesting because the merging between two nodes located at the diagonal corners of a square is possible (nodes located at distance $d=\sqrt{2}$ in the original lattice) leading to link merging [32]. Thus, we need to introduce a term, $\pi_{\sqrt{2}}(\delta,\epsilon)$, which accounts for the diagonal merging. To obtain $\pi_{\sqrt{2}}(\delta,\epsilon)$, we need to introduce in Eq. (6) the following values:

$$\int_{v_i\cup v_j} dv = \frac{4}{3}\pi(\epsilon+\delta)^3+\frac{4}{3}\pi\delta^3-\int_{v_i\cap v_j} dv,$$

$$\int_{v_i\cap v_j} dv = \frac{\pi}{12\sqrt{2}}(2\delta+\epsilon-\sqrt{2})^2\times(2+4\sqrt{2}\delta+2\sqrt{2}\epsilon-3\epsilon^2).$$

Now the expected number of nodes will be

$$N(\delta,\epsilon)\sim[1-\pi_1(\delta,\epsilon)-\pi_{\sqrt{2}}(\delta,\epsilon)]HS^2, \tag{13}$$

and the expected number of links will be

$$|E(p,q)|=[1-\pi_{\sqrt{2}}(\delta,\epsilon)][(2p+q)HS^2-2pHS-qS^2]. \tag{14}$$

This results, again, in a linear behavior on $x=4p+2q$ of the leading term of $\langle k\rangle$,

$$\langle k\rangle\approx\frac{[1-\pi_{\sqrt{2}}(\delta,\epsilon)]}{1-\pi_1(\delta,\epsilon)-\pi_{\sqrt{2}}(\delta,\epsilon)}x+\mathcal{O}\left(\frac{1}{S}+\frac{1}{H}\right). \tag{15}$$

Higher values of $2\delta+\epsilon$ will increase both node merging and link fusion, but we stop our analysis here since the above approximation is enough for our purposes.

By comparing these theoretical predictions with real data, we can see that the linear form (after $4p+2q\geq 2$) is found in the simulated webs by computing the size of the largest connected component against $4p+2q$. In Fig. 8 we show the numerical results where obtained through numerical simulation by taking 20 sample networks for every pair (p,q), with $p\in[0,1]$, $q\in[0,1]$ (2000 networks per plot) and the parameters δ and ϵ were fixed to the best fitting parameters in Table I. For each data set, we also estimate the position of the network expected connectivity and, as we can see, they all fall very close to the percolation threshold. An exception is data set $c19$, which is consistent with the fact that is an unfinished set and thus will have larger numbers of links [8].

VI. GLOBAL EFFICIENCY

An important feature of the nest is their ability to sustain an active colony of termites. This is actually closely related to network's navigability [33]. We have conjectured that Cubitermes nests are efficient transportation networks in spite of their sparseness [34]. Here, we assess network efficiency by comparing $E_{loc}(G)$ and $E_{glob}(G)$ (16) measured in the real nests to the predictions from our lattice model. The topological efficiency of synthetic and real networks [35] is here measured by

$$E(G)=\frac{1}{N(N-1)}\sum_{i\cong j}\frac{1}{D(i,j)}. \tag{16}$$

From the above definition, we can compute the local network efficiency or the global network efficiency. We can compute the local topological efficiency at every node i with the subgraph G_i of the neighbors of i. Moreover, we define local efficiency as the average efficiency of the local subgraphs, $E_{loc}(G)=1/N\Sigma_{i\in G}E(G_i)$. On the other hand, the global efficiency $E_{glob}(G)$ measures the topological efficiency in the whole graph G.

The model gives good predictions for the local and global efficiencies (see Fig. 9). In spite that these nests exhibit some

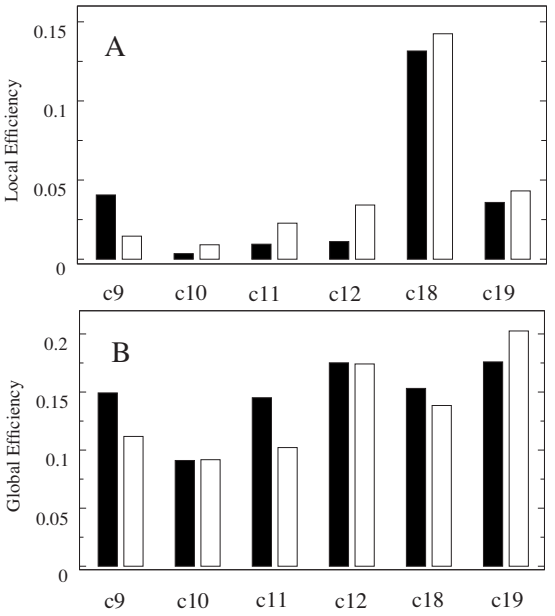

FIG. 9. Comparison between E_{loc} and E_{glob} in the real networks (black bars) and the model networks (white bars). (a) Local efficiency. (b) Global efficiency. Efficiency values in the model have been averaged over 1000 networks with the best fitting parameters.

significant variability, a very good agreement was obtained. The model overestimates local efficiency for the networks $c10, c11, c12$ and underestimates the global efficiency for the same networks. We can explain this as a consequence of the natural balance between local and global efficiencies taking place in sparse networks. The model also overestimates both the local and global efficiencies for nest $c19$ partly because of the relatively large network connectivity, i.e., $\langle k \rangle = 3.25$ is the largest average degree of the six networks analyzed here.

VII. DISCUSSION

In this paper we have analyzed the organization of layered insect nests, showing that their architecture is consistent with an optimal network. Specifically, using both data from real termite nests and a disordered lattice model, we provided evidence for a link minimization process. The networks representing termite nests are shown to be close to the percolation threshold, thus allowing to properly span the entire nest volume at a low cost. This has been shown to be consistent with the efficiency measures and suggests that the rules of nest construction have been optimized through evolution in order to maximize network functionality while minimizing its connectivity.

ACKNOWLEDGMENTS

We thank Christian Jost for useful comments. We also thank Jacques Gautrais, Stéphane Douady, and Stephanie Widder for useful discussions. S.V. was supported by a research grant from the MESOMORPH project (Grant No. ANR-06-BYOS-0008). R.V.S. was supported by Ministerio de Ciencia y Tecnología (MCyT), Research Grant No. FIS2004-05422, by the James McDonnell Foundation, and by the Santa Fe Institute.

[1] S. J. Gould, *The Structure of Evolutionary Theory* (Belknap, Harvard, 2002).
[2] *Scaling in Biology*, edited by J. H. Brown and G. B. West (Oxford University Press, New York, 2000).
[3] D. B. Chklovskii, T. Schikorski, and C. Stevens, Neuron **34**, 341 (2002).
[4] C. Cherniak, Neuroscience **18**, 522 (1995).
[5] R. Durbin and G. Mitchinson, Nature (London) **343**, 644 (1990).
[6] G. Theraulaz, E. Bonabeau, and J.-L. Deneubourg, Complexity **3**, 15 (1998).
[7] J. Korb, Curr. Biol. **17**, R995 (2007).
[8] A. Perna, C. Jost, E. Couturier, S. Valverde, S. Douady, and G. Theraulaz, Naturwiss. **95**, 877 (2008).
[9] E. Bonabeau, Artif. Life **5**, 95 (1999).
[10] S. Camazine, J.-L. Deneubourg, N. R. Franks, J. Sneyd, G. Theraulaz, and E. Bonabeau, *Self-organization in Biological Systems* (Princeton University Press, Princeton, 2003).
[11] *Information Processing in Social Insects*, edited by C. Detrain, J.-L. Deneubourg, and J. M. Pasteels (Brikhauser, Basel, 1999).
[12] D. J. Watts and S. H. Strogatz, Nature (London) **393**, 440 (1998).
[13] S. N. Dorogovtsev and J. F. F. Mendes, *Evolution of Networks: From Biological Nets to the Internet and WWW* (Oxford University Press, New York, 2003).
[14] P. Sen, S. Dasgupta, A. Chatterjee, P. A. Sreeram, G. Mukherjee, and S. S. Manna, Phys. Rev. E **67**, 036106 (2003); N. Mathias and V. Gopal, *ibid.* **63**, 021117 (2001); R. F. Cancho, C. Janssen, and R. V. Sole, *ibid.* **64**, 046119 (2001).
[15] J. Buhl, J. Gautrais, N. Reeves, R. V. Solé, S. Valverde, P. Kuntz, and G. Theraulaz, Eur. Phys. J. B **49**, 513 (2006); J. Buhl, J. Gautrais, R. V. Solé, P. Kuntz, S. Valverde, J. L. Deneubourg, and G. Theraulaz, *ibid.* **42**, 123 (2004).
[16] M. F. Bear, B. W. Connors, and M. A. Paradiso, *Neuroscience* (Williams and Williams, Baltimore, 1996).
[17] D. M. L. Cooper, A. L. Turisnky, C. W. Sensen, and B. Hallgrimsson, Anat. Rec. **274B**, 169 (2003).
[18] M. P. Viana, E. Tanck, M. E. Beletti, and L. F. Costa, Mol. BioSyst. **5**, 255 (2009).
[19] T. Hogg, Y. Chen, and P. J. Kuekes, IEEE Trans. Nanotechnol. **5**, 110 (2006).
[20] P. Iniesto, J. Deligne, G. Josens, and J. Verbanck, Actes Coll. Insectes Sociaux **14**, 39 (2001).
[21] G. Voronoi, J. Reine Angew. Math. **134**, 198 (1908).
[22] I. Dayan, J.-F. Gouyet, and S. Havlin, J. Phys. A **24**, L287 (1991).
[23] J. Buhl, J. Gautrais, J.-L. Deneubourg, P. Kuntz, and G. Theraulaz, J. Theor. Biol. **243**, 287 (2006).
[24] P. P. Grassé, *Termitologia, Tome II: Foundation des Sociétés,*

Construction (Masson, Paris, 1984).
[25] J. P. E. C. Darlington, J. Zool. **198**, 237 (1982).
[26] J.-A. Lys and R. H. Leuthold, Insectes Soc. **38**, 63 (1991).
[27] S. Gottschalk, M. C. Lin, and D. Manocha, *Proceedings of the 23th Conference on Computer Graphics International Technology (SIGGRAPH)* (ACM, New York, 1996), pp. 171–180.
[28] J. Marin and R. V. Solé, IEEE Trans. Evol. Comput. **3**, 272 (1999); Phys. Rev. E **65**, 026207 (2002).
[29] P. W. Holland and S. Leinhardt, Am. J. Sociol. **76**, 492 (1970).
[30] A. Vazquez, A. Flammini, A. Maritan, and A. Vespignani, ComPlexUs **1**, 38 (2003).
[31] S. Wernicke, IEEE/ACM Trans. Comput. Biol. Bioinf. **3**, 347 (2006).
[32] Imagine a square where merging is performed among the two nodes of a given diagonal. Then, from a square we will obtain a chain of three elements, thus loosing two links, which have been fusioned.
[33] J. M. Kleinberg, Nature (London) **406**, 845 (2000).
[34] A. Perna, S. Valverde, J. Gautrais, C. Jost, R. Solé, P. Kuntz, and G. Theraulaz, Physica A (to be published).
[35] V. Latora and M. Marchiori, Phys. Rev. Lett. **87**, 198701 (2001).